View metadata, citation and similar papers at core.ac.uk

brought to you by CORE

provided by University of Kentucky

University of Kentucky
UKnowledge

Civil Engineering Faculty Publications

Civil Engineering

3-15-2018

Bio-Inspired Hybrid Vibration Control Methodology for Intelligent Isolated Bridge Structures

Mariantonieta Gutierrez Soto
University of Kentucky, mariant.gutierrezsoto@uky.edu

Right click to open a feedback form in a new tab to let us know how this document benefits you.

Follow this and additional works at: https://uknowledge.uky.edu/ce_facpub

Part of the Civil Engineering Commons, and the Structural Engineering Commons

Repository Citation

Soto, Mariantonieta Gutierrez, "Bio-Inspired Hybrid Vibration Control Methodology for Intelligent Isolated Bridge Structures" (2018). *Civil Engineering Faculty Publications*. 11.
https://uknowledge.uky.edu/ce_facpub/11

This Conference Proceeding is brought to you for free and open access by the Civil Engineering at UKnowledge. It has been accepted for inclusion in Civil Engineering Faculty Publications by an authorized administrator of UKnowledge. For more information, please contact UKnowledge@lsv.uky.edu.

Bio-Inspired Hybrid Vibration Control Methodology for Intelligent Isolated Bridge Structures

Notes/Citation Information
Published in *Proceedings of SPIE*, v. 10595, Active and Passive Smart Structures and Integrated Systems XII, article 1059511, p. 1-13.

© 2018 SPIE. One print or electronic copy may be made for personal use only. Systematic reproduction and distribution, duplication of any material in this publication for a fee or for commercial purposes, and modification of the contents of the publication are prohibited.

Mariantonieta Gutierrez Soto, "Bio-inspired hybrid vibration control methodology for intelligent isolated bridge structures," *Proc. SPIE* 10595, Active and Passive Smart Structures and Integrated Systems XII, 1059511 (March 15, 2018). DOI: https://doi.org/10.1117/12.2300393

The copyright holder has granted the permission for posting the article here.

Digital Object Identifier (DOI)
https://doi.org/10.1117/12.2300393

This conference proceeding is available at UKnowledge: https://uknowledge.uky.edu/ce_facpub/11

PROCEEDINGS OF SPIE

SPIEDigitalLibrary.org/conference-proceedings-of-spie

Bio-inspired hybrid vibration control methodology for intelligent isolated bridge structures

Mariantonieta Gutierrez Soto

Mariantonieta Gutierrez Soto, "Bio-inspired hybrid vibration control methodology for intelligent isolated bridge structures," Proc. SPIE 10595, Active and Passive Smart Structures and Integrated Systems XII, 1059511 (15 March 2018); doi: 10.1117/12.2300393

SPIE.

Event: SPIE Smart Structures and Materials + Nondestructive Evaluation and Health Monitoring, 2018, Denver, Colorado, United States

Downloaded From: https://www.spiedigitallibrary.org/conference-proceedings-of-spie on 15 Mar 2019 Terms of Use: https://www.spiedigitallibrary.org/terms-of-use

Bio-inspired hybrid vibration control methodology for intelligent isolated bridge structures

Mariantonieta Gutierrez Soto[a]

[a]University of Kentucky, 161 Oliver H. Raymond Building, Lexington, KY, U.S.A.

ABSTRACT

Inspired by evolutionary game theory, the biological game of replicator dynamics is investigated for vibration control of bridge structures subjected to earthquake excitations. Replicator dynamics can be interpreted economically as a model of imitation of successful individuals. This paper uses replicator dynamics to reduce vibrations while optimally allocating the control device forces. The control algorithm proposed is integrated with a patented neural dynamic optimization algorithm to find optimal growth rate values with the goal of achieving satisfactory structural performance with minimum energy consumption. A model is described for hybrid vibration control of smart highway bridge structures subjected to earthquake loading.

Keywords: Game theory, smart structures, vibration control, replicator dynamics, bio-inspired, bridge, earthquake

1. INTRODUCTION

1.1 Problem Statement

The investigation of innovative mitigation strategies for protection of civil structures is motivated by the current trend of more flexible structures, higher safety demand, more stringent performance criteria and better use of materials and economic considerations. Furthermore, the American Society of Civil Engineers' Report Card of America's civil infrastructure as "D+" that stands in the category for "Poor, At Risk" condition and mostly below standard. The U.S. has 614,387 bridges and four in 10 of which are 50 years or older. In addition, 188 million trips are taken every day across structurally deficient bridges. A survey of over 500 bridge failures in the US over the range 1989-2000 showed a total of 17 bridges failing during historical major earthquake events. Highway bridge structures are critical during extreme events. The implications of a bridge structure compared with a building structures during a natural disaster varies. If a highway bridge structure collapses, communities could be disconnected and create a challenge for evacuation and also for first responders to access the site. It will also significantly impede the short-term recovery after a natural disaster. Although new technologies and materials have improve the maintenance to extend the bridge life, most of these innovations do not include the adaptability during extreme events. Environmental loads such as earthquake and wind loadings are highly uncertain and unpredictable which gives urgency for reconfigurable strategies that can make a structure adapt in real-time.

1.2 Smart Highway Bridge Structures

The field of structural control can be classified into passive control, active control and semi-active control. Passive control has characteristics of non-controllable and no power requirement. Examples include passive fluid viscous dampers, base isolation and tuned mass dampers. In the last 20 years, investigations leading to adding damping devices have gained interest in current bridge engineering practice. A key case study integrating isolation bearings and passive fluid viscous dampers in a highway bridge structure located in California can be found in Makris and Zhang (2004). More recently, AASHTO reported over 200 bridges designed by 2011 with seismic isolation in the US and around the world. Active control is controllable and requires significant power requirement. Examples of

Further author information: (Send correspondence to M.G.S.)
M.G.S.: E-mail: mariant.gutierrezsoto@uky.edu, Telephone: 1 859-257-1855

Active and Passive Smart Structures and Integrated Systems XII, edited by Alper Erturk, Jae-Hung Han,
Proc. of SPIE Vol. 10595, 1059511 · © 2018 SPIE · CCC code: 0277-786X/18/$18 · doi: 10.1117/12.2300393

Downloaded From: https://www.spiedigitallibrary.org/conference-proceedings-of-spie on 15 Mar 2019
Terms of Use: https://www.spiedigitallibrary.org/terms-of-use

active structural control devices include active bracings, active mass dampers and linear actuators. The concept of active control of civil structures started by J. T. P. Yao in 1972. An external source supplies power to the actuator to apply forces to the structure. These forces are determined by a control algorithm and can be used to both add and dissipate energy in the structure. Semi-active control is the fusion of passive and active control in that it has the control ability and has little power requirement. A smart highway bridge investigated in this paper is instrumented with sensors and hybrid damping using a combination of semi-active devices (MR dampers) with passive devices (isolation bearings) is shown in Figure 1.

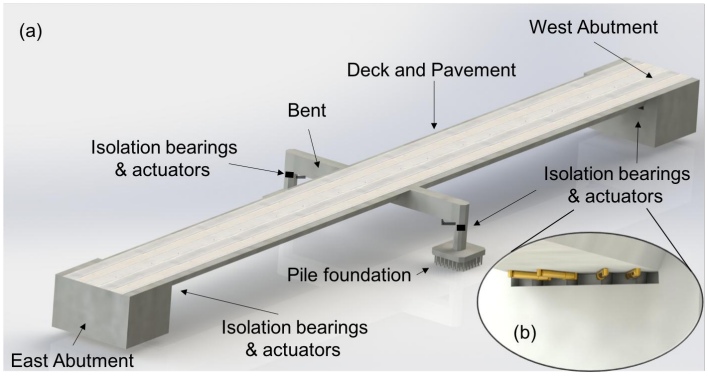

Figure 1. Three-dimensional view of bridge structure equipped with isolation bearings and control devices.

1.3 Equations of Motion

The equations of motion of the structural bridge equipped with hybrid control system containing an active/semi-active and passive control systems subjected to earthquake loads is described mathematically as:

$$\mathbf{M}\ddot{\mathbf{u}}(t) + \mathbf{C}\dot{\mathbf{u}}(t) + \mathbf{K}\mathbf{u}(t) = -\mathbf{M}\eta\ddot{\mathbf{u}}_g(t) + \mathbf{G}\mathbf{g}(t) + \mathbf{H}\mathbf{h}(t) \tag{1}$$

where $\mathbf{M}$, $\mathbf{C}$, and $\mathbf{K}$ are the assembled mass, damping and stiffness matrices of the bridge. Vector η is the influence vector of the external force (ground acceleration) and $\ddot{\mathbf{u}}_\mathbf{g}(\mathbf{t})$ is the ground acceleration vector in both directions. $\mathbf{G}$ and $\mathbf{H}$ the influence matrices for the control forces, and vectors $\mathbf{g}(t)$ and $\mathbf{h}(t)$ contains the control forces generated by the passive and active control devices, respectively. Equation 1 is transformed into the state space model representation as follows:

$$\dot{\mathbf{x}}(t) = \mathbf{A}\mathbf{x}(t) + \mathbf{B}_\mathbf{b}\mathbf{z}_\mathbf{b}(t) + \mathbf{B}_\mathbf{c}\mathbf{z}_\mathbf{c}(t) + \mathbf{E}\ddot{\mathbf{u}}_\mathbf{g}(t) \tag{2}$$

$$\mathbf{y}(t) = \mathbf{C}\mathbf{x}(t) + \mathbf{D}\mathbf{z}(t) + \mathbf{L}\ddot{\mathbf{u}}_\mathbf{g}(t) + \mathbf{v} \tag{3}$$

where $\mathbf{A}$, $\mathbf{E}$, $\mathbf{C}$, $\mathbf{D}$ and are the state-space matrices and $\mathbf{x}$ is the state vector of the structural system and $\mathbf{y}$ is the vector of measured outputs. $\mathbf{B_b}$ and $\mathbf{B_c}$ are matrices of the control device forces, and $\mathbf{v}$ is the noise measurement vector.

The passive control isolation system is modeled using the bilinear force-deformation in the x and y axis direction using formulae:

$$\mathbf{g_x} = \mathbf{K_{px}}\mathbf{u_x} + (\mathbf{K_{ex}} - \mathbf{K_{px}})\bar{\mathbf{u}}_\mathbf{bx} \tag{4}$$

$$\mathbf{g_y} = \mathbf{K_{py}}\mathbf{u_y} + (\mathbf{K_{ey}} - \mathbf{K_{py}})\bar{\mathbf{u}}_\mathbf{by} \tag{5}$$

where $\bar{\mathbf{u}}_\mathbf{bx}$ and $\bar{\mathbf{u}}_\mathbf{by}$ are the yield displacements of the bearings, $\mathbf{g_x}$ and $\mathbf{g_y}$ are the restoring forces of the bearing in the x and y directions, respectively. $\mathbf{K_{px}}$, $\mathbf{K_{py}}$, $\mathbf{K_{ex}}$ and $\mathbf{K_{ey}}$ are constant stiffness parameters.

Downloaded From: https://www.spiedigitallibrary.org/conference-proceedings-of-spie on 15 Mar 2019
Terms of Use: https://www.spiedigitallibrary.org/terms-of-use

2. BIO-INSPIRED CONTROL ALGORITHM: EVOLUTIONARY DYNAMICS

The concept of evolution in biological studies has been a source of inspiration that transcends across many fields of study. The concept of evolution requires populations of reproducing individuals. The evolutionary change occurs by mutation and selection processes. Selection takes places during competition of groups with different fitness. Let us look at a survival of the fittest example where a group A has fitness of 1 and a B individual has a fitness of 1.1. In this case, the fitness of B out-competes the fitness of A and in time, every individual in group A will convert to B. In general, the fitness landscape changes as the population moves across time and it leads to the concept of evolutionary game theory. Fitness depends on the relative abundance of different types. One concept of evolutionary game theory is the replicator dynamics, also known as population dynamics, that occurs when successful strategies spread by natural selection. This biological modeling has been studied for mosquitoes control, as well as across boundaries to model economics, changes of political parties in a population, or shifts in social behaviors.

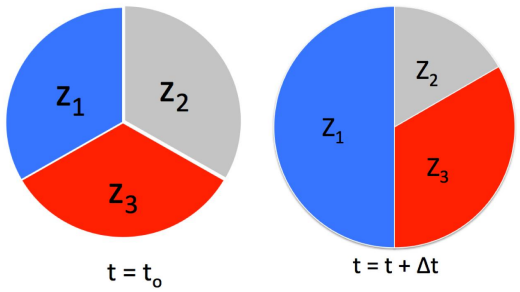

Figure 2. Replicator dynamics approach for room temperature control

Populations dynamics was investigated in electrical engineering to model the resource allocation for temperature control.[1] Figure 2 shows an example of replicator dynamics approach for temperature control. At a initial time, $t = t_o$, three different zones, $z_1(t), z_2(t)$ and $z_3(t)$, have equal distribution of resources. The total sum of these resources is the total population, $z_1(t) + z_2(t) + z_3(t) = P$. At a later time, $t = t + \Delta t$, an user in the first zone z_1 desired a colder temperature $T(t + \Delta t)$, which in turn, required additional resources allocated to $z_1(t + \Delta t$ to reach the new temperature. As depicted in the figure, the total resources are distributed among the zones, but the total resources, or total population, P remains the same. The amount of resources given to the zones is determined by a fitness function for each zone $f_i(t, T) = T_i(t)$ and $f_i(t, T) > 0$. Combining these variables, the populations dynamics equation also known as the replicator ecology equation is formulated as:

$$\dot{z}_i(t) = z_i(t) \left[f_i(t, T) - \phi(t, T, f) \right] \tag{6}$$

The weighed average fitness function or payoff formulated as:

$$\phi(t, T) = \frac{1}{P} \sum_{i=1}^{N} z_i(t) f_i(t, T) \tag{7}$$

This bio-inspired algorithm is adapted as a resource allocation algorithm for active and semi-active vibration control of structures such as high-rise building structures subjected to earthquake loadings.[2] This paper introduces the concept for vibration control of highway bridge structures. Figure 3 shows the schematic of the proposed population dynamic control algorithm presented in this paper.

The smart bridge structure is instrumented with control devices. The manner in which these forces are allocated to each control device is done using replicator dynamics. Each zone represents the forces allocated to each control devices. The total population are the total available resources or control forces that can be distributed to the control devices. Instead of temperature measurements used in the fitness function, the sensor measurements are displacement and acceleration. There are additional considerations for stability of the replicator dynamics:

Downloaded From: https://www.spiedigitallibrary.org/conference-proceedings-of-spie on 15 Mar 2019
Terms of Use: https://www.spiedigitallibrary.org/terms-of-use

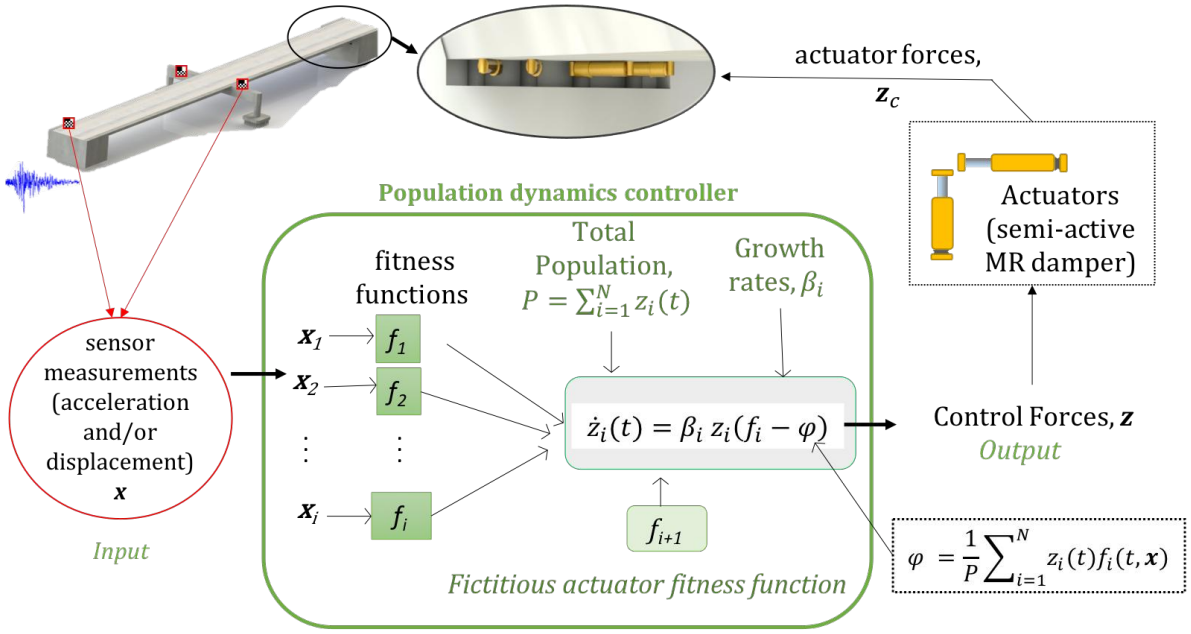

Figure 3. Bio-inspired approach of population dynamics for active/semi-active vibration control of bridge structures

1. The fitness function in population dynamics has to be strictly positive. The bridge will have negative measurements (displacement or accelerations acting in the opposite direction) and it will have to be accounted for in the formulation of the new model.

2. In the event that there is no substantial displacement or acceleration, the resources should be allocated somewhere to maintain the populations dynamics. Therefore, a *fictitious* control device, $z_{n+1}(t)$ is added to the populations dynamic algorithm to capture the excess resources. These also allows for limitation of power consumption.[1]

3. The rate in which the resources are distributed among control devices. This is done in population dynamics by adding a growth rate variable β[3] to the replicator dynamics equation.

Adding the growth rate variables and deriving the model for 3D structural models revises equation 6 to:

$$\dot{z}_{xi}(t) = \beta_x z_{xi}(t)\left[f_{xi}(t, \mathbf{x}) - \phi_x(t, \mathbf{x}, \mathbf{f})\right] \tag{8}$$

$$\dot{z}_{yi}(t) = \beta_y z_{yi}(t)\left[f_{yi}(t, \mathbf{x}) - \phi_y(t, \mathbf{x}, \mathbf{f})\right] \tag{9}$$

The fitness functions for each control device is formulated as:

$$f_{xi}[t, \mathbf{y}(t)] = \begin{cases} \max\left[u_{xi}(t), d_{xi}\right] & u_x(t) > 0 \quad \forall i = 1, 2, \ldots N \\ \max\left[-u_{xi}(t), d_{xi}\right] & u_x(t) < 0 \quad \forall i = 1, 2, \ldots N \end{cases} \tag{10}$$

$$f_{yi}[t, \mathbf{y}(t)] = \begin{cases} \max\left[u_{yi}(t), d_{yi}\right] & u_y(t) > 0 \quad \forall i = 1, 2, \ldots N \\ \max\left[-u_{yi}(t), d_{yi}\right] & u_y(t) < 0 \quad \forall i = 1, 2, \ldots N \end{cases} \tag{11}$$

where d_{xi} and d_{yi} are the desired displacement for i^{th} location along the x-axis and y-axis respectively. Similar approach can be taken if the desired control decisions are based on the measured base shear, overturning moment, mid-span acceleration, bearing deformation with respect to the corresponding desired performance value.

Downloaded From: https://www.spiedigitallibrary.org/conference-proceedings-of-spie on 15 Mar 2019
Terms of Use: https://www.spiedigitallibrary.org/terms-of-use

Depending on the fitness function, the control designer has to determine the appropriate growth rate value. The growth rate values could be obtained using extensive parametric numerical simulations, or via optimization. The approach investigated in this paper modifies the robust patented Neural Dynamic model of Adeli and Park[4] to determine the optimal growth rate values for the population dynamics controller.

3. BIO-INSPIRED OPTIMIZATION ALGORITHM: NEURAL DYNAMICS MODEL

Neural networks have been used extensively in artificial intelligence to model computation learning. It has also been a popular soft computing algorithm approach to solve optimization problems. Traditional neural networks optimization have a tendency to land local optima solution. However, the patented Neural Dynamic Model of Adeli and Park overcomes such limitations and was created to solve a discrete optimization problem for minimum weight design of three large space steel structures ranging in size from 1,310 to 8,904 members.[5] It was proven to be effective in managing nonlinear constraints and able to achieve global optimum with a substantial reduction in computational requirement. Gutierrez and Adeli extended the idea presented for many-objective optimization approach to obtain Pareto-optimal design parameters of a controller that reduce vibrations of high-rise buildings subjected to 2,500 earthquake loadings.[6] This model was also investigated for vibration control of smart base isolated structures.[7]

3.1 General Mathematical Optimization

An optimization problem in general as a minimization of an objective function:

$$F(\theta) \tag{12}$$

subject to the following constraints:

$$g_j(\theta) \leq 0 \text{ for } j = 1, 2, ..., G \tag{13}$$

$$h_k(\theta) = 0 \text{ for } k = 1, 2, ..., H \tag{14}$$

where θ has the design variables, $g_j(\theta)$ is the jth inequality constraint function, $h_k(\theta)$ is the kth equality constraint function, G is the total number of inequality constraints, and H is the total number of equality constraints.

3.2 NDAP Derivation Bridge Replicator Control Parameter Optimization

The replicator control parameters are the design variables of the optimization problem that regulates how the control decisions are computed to reduce vibrations of the bridge structure subjected to earthquake loadings.

Figure 4 shows the topology of the neural dynamics model.[4] Let θ define the vector of design variables, $\theta = [\beta_{ix}\beta_{iy}, \beta_{n+1}, P, f_{n+1}]$. The design objectives for this problem are to minimize structural performance in x and y directions. The structural performance is decided by the control designer and can be base shear, overturning moment, mid-span acceleration, bearing deformation, etc. The objective function used in this research paper is to minimize $(\theta) = [\mathbf{F_x}\mathbf{F_y}]$ the following:

$$\mathbf{F_x}(\theta) = \max_{i,t} \|\ddot{u}_{xi}\|^2 \text{ for } i = 1, 2, ..., N \tag{15}$$

$$\mathbf{F_y}(\theta) = \max_{i,t} \|\ddot{u}_{yi}\|^2 \text{ for } i = 1, 2, ..., N \tag{16}$$

subject to

$$|z_j| \leq z_{max} \text{ for } r = 1, ..., R \tag{17}$$

where z_{max} is the maximum force capacity of the actuator.

$$g_1(\theta) : |z_j| - z_{max} \leq 0 \text{ for } r = 1, ..., R \tag{18}$$

Downloaded From: https://www.spiedigitallibrary.org/conference-proceedings-of-spie on 15 Mar 2019
Terms of Use: https://www.spiedigitallibrary.org/terms-of-use

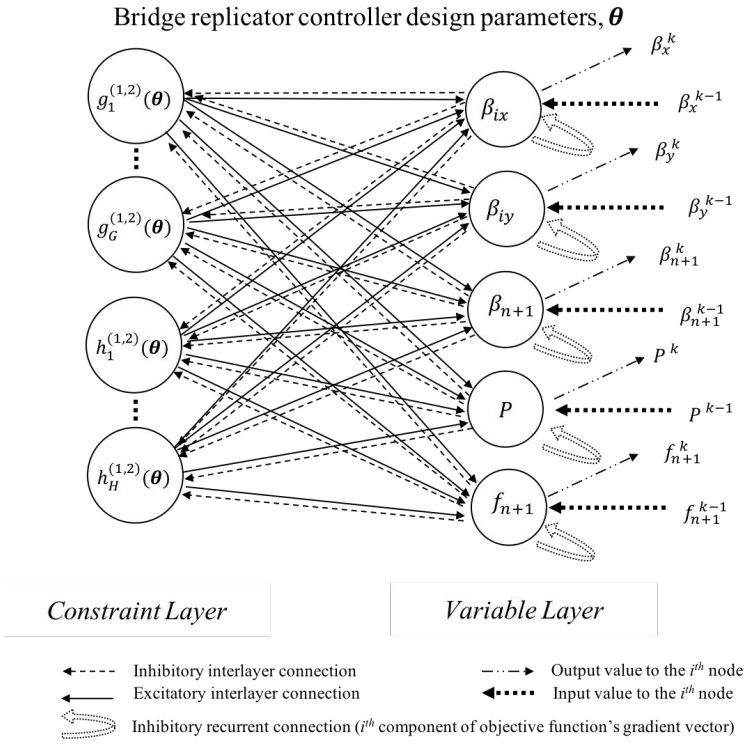

Figure 4. Topology of neural dynamics model for vibration control of smart bridge structure

$$g_2(\theta) : -\beta_{ix} < 0 \text{ for } r = 1, ..., R \tag{19}$$

$$g_3(\theta) : \beta_{ix} - \beta_{max} \leq 0 \text{ for } r = 1, ..., R \tag{20}$$

where β_{max} is the maximum growth rate parameter which describes the control decision response or *slowness* of the control device and it is problem dependent.

$$g_4(\theta) : \mathbf{J}(\theta) - \mathbf{J}_{max} < 0 \tag{21}$$

where $\mathbf{J}$ is the normalized performance criteria (described in the evaluation section of this paper) and compared with the maximum desired value.

The Lyapunov stability theorem is satisfied for the neural dynamic model by:

$$\dot{\theta} = -\nabla \mathbf{F}(\theta) - \alpha_p \left[\sum_{j=1}^{G} g_j^+(\theta) \nabla g_j^+(\theta) + \sum_{k=1}^{H} h_k(\theta) \nabla h_k^+(\theta) \right] \tag{22}$$

where α_p is the exterior penalty function that changes at each iteration and is computed as:

$$\alpha_p = \alpha_0 + \frac{p}{\epsilon} \tag{23}$$

where α_0 is the initial penalty function that increases until it reaches the p iterations and $\epsilon > 0$ dependent on the optimization problem.

The equilibrium point is obtained by applying the Runge-Kutta Method to integrate numerically the following:

$$\theta = \int \dot{\theta} \tag{24}$$

Downloaded From: https://www.spiedigitallibrary.org/conference-proceedings-of-spie on 15 Mar 2019
Terms of Use: https://www.spiedigitallibrary.org/terms-of-use

where θ contains the control algorithm design variables. The vector $\theta^{\star}$ to be a local optimum solution where the Kuhn-Tucker conditions in Eqns. 18 - 21 must be satisfied.

4. APPLICATION

The seismic behavior of the interstate California State Route 91 (abbreviated as 91/5) overcrossing highway bridge in southern California has been the subject of significant research because it is installed with passive dampers. The analysis of the case study is described in.[8]

The bridge has a reinforced concrete deck supported near the center span with a prestressed reinforced concrete bent with two earth embankments at the two ends. As a case study, this bridge has been equipped with eight fluid dampers and four elastomeric bearings at each end that connect the deck with the abutment to aid the vibration reduction.

Figure 5. (a) Hydraulic dampers installed in the bridge case study. (b) Google street view of the actual highway bridge

Figure 5 shows a street view of the actual highway bridge along with a close-up showing the passive hydraulic dampers installed in the 91/5 overcrossing highway bridge located in California ($33°51'27.5"$ N $117°58'46.9"W$). In this paper, the hydraulic dampers are substituted with semi-active magneto-rheological dampers. The transverse and longitudinal periods of the bridge structure are in the range between 0.4s and 0.8s; which makes additional supplemental damping can be effective.

Agrawal et al.[9] created a highway benchmark control problem based on the 91/5 overcrossing highway bridge model subjected to historical earthquakes for the purpose of evaluating the performance of existing and new control algorithms. Figure 6 shows the plan view of the benchmark problem showing location of sensors and control devices. The bridge plan depicts the locations of 12 semi-active MR dampers noted along the x and y direction, and the 10 nonlinear elastomeric bearings with a lead core isolation system. The full structural finite element model (FEM) has 430 DOF.

Downloaded From: https://www.spiedigitallibrary.org/conference-proceedings-of-spie on 15 Mar 2019
Terms of Use: https://www.spiedigitallibrary.org/terms-of-use

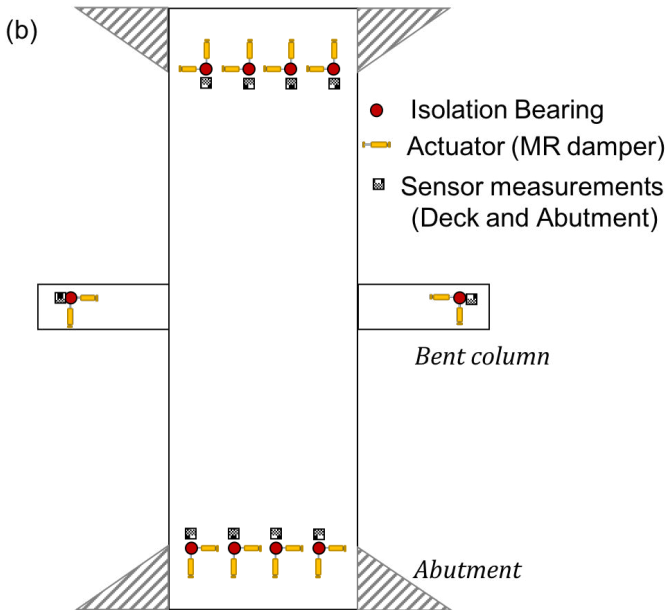

Figure 6. Plan view of the benchmark problem showing location of sensors and control devices

5. EVALUATION

5.1 Historical earthquakes

The benchmark problem is evaluated by subjecting the structure to major historical earthquakes.

1. The 1986 North Palm Springs earthquake that affected northern Owens Valley and Southern California with a magnitude of Mw = 6.0.
2. The 1999 Chi-Chi earthquake in Taiwan with a magnitude of Mw =7.6, station TCU 084
3. The 1940 Imperial Valley Earthquake with a magnitude of Mw = 6.4, El Centro component
4. The 1994 Northridge earthquake at the Rinaldi station with a magnitude of Mw = 6.7
5. The 1999 Dzce earthquake in Turkey with a magnitude of Mw = 7.2, the Bolu component
6. The 1995 Great Hanshin-Awaji (Kobe) earthquake in Japan with a magnitude of Mw = 6.9

5.2 Performance Criteria for Isolated Highway Bridge Structure

The benchmark problem is evaluated using performance criteria for maximum base shear (J1), maximum overturning moment (J2), maximum midspan displacement (J3), maximum acceleration (J4), bearing deformation (J5), maximum curvature or ductility (J6), maximum root mean square (RMS) of base shear (J9), and maximum RMS of base moment (J10), maximum RMS of midspan displacement (J11), maximum RMS of midspan acceleration (J12), maximum RMS of abutment displacement (J13), and maximum RMS of ductility (J14). The control system performance criteria is defined for peak control force (J15), device stroke (J16) and instantaneous power (J17). The following is the performance criteria used to evaluate performance for each earthquake. The denominator contains the response quantity of the "uncontrolled" case, which is only with passive isolation system.

J_1 is the normalized maximum shear of the controlled structure divided by the corresponding maximum uncontrolled shear response, ${V_b}^{max} = |V_{uncontrolled}(t)|$.

$$J_1 = \max_t = \frac{|V_b(t)|}{{V_b}^{max}} \tag{25}$$

Downloaded From: https://www.spiedigitallibrary.org/conference-proceedings-of-spie on 15 Mar 2019
Terms of Use: https://www.spiedigitallibrary.org/terms-of-use

J_2 is the maximum overturning moment of the controlled structure divided by the corresponding maximum uncontrolled overturning moment.

$$J_2 = \max_t = \frac{|M_b(t)|}{{M_b}^{max}} \tag{26}$$

J_3 is the maximum mid-span displacement of the controlled structure, $u_m(t)$ divided by the maximum uncontrolled mid-span displacement.

$$J_3 = \max_t = \frac{|u_m(t)|}{{u_m}^{max}} \tag{27}$$

J_4 is the maximum mid-span acceleration of the controlled structure, $\ddot{u}_m(t)$ divided by the maximum uncontrolled mid-span acceleration.

$$J_4 = \max_t = \frac{|\ddot{u}_m(t)|}{\ddot{u}_m^{max}} \tag{28}$$

J_5 is the maximum bearing deformation of the controlled structure, $u_b(t)$ divided by the maximum uncontrolled bearing deformation.

$$J_5 = \max_t = \frac{|\ddot{u}_m(t)|}{\ddot{u}_m^{max}} \tag{29}$$

J_6 defines the maximum column curvature of the controlled structure, $\phi(t)$ divided by the maximum uncontrolled column curvature:

$$J_6 = \max_t = \frac{|\phi(t)|}{\phi^{max}} \tag{30}$$

The following criteria are normalized using the root-mean-squared (RMS) approach, $\|x\| = \sqrt{x^2}$.

J_9 is the RMS of the maximum shear of the controlled structure divided by the corresponding RMS of the maximum uncontrolled shear response, $\|{V_b}^{max}\| = \|V_{uncontrolled}(t)\|$.

$$J_9 = \max_t = \frac{\|V_b(t)\|}{{V_b}^{max}} \tag{31}$$

J_{10} is the RMS of the maximum overturning moment of the controlled structure divided by the corresponding RMS of the maximum uncontrolled overturning moment.

$$J_{10} = \max_t = \frac{\|M_b(t)\|}{\|{M_b}^{max}\|} \tag{32}$$

J_{11} is the RMS of the maximum mid-span displacement of the controlled structure, $u_m(t)$ divided by the RMS of the maximum uncontrolled mid-span displacement.

$$J_{11} = \max_t \frac{\|u_m(t)\|}{\|{u_m}^{max}\|} \tag{33}$$

J_{12} is the RMS of the maximum mid-span acceleration of the controlled structure, $\ddot{u}_m(t)$ divided by the RMS of the maximum uncontrolled mid-span acceleration.

$$J_{12} = \max_t \frac{\|\ddot{u}_m(t)\|}{\|\ddot{u}_m^{max}\|} \tag{34}$$

J_{13} is the RMS of the maximum bearing deformation of the controlled structure, $u_b(t)$ divided by the RMS of the maximum uncontrolled bearing deformation.

$$J_{13} = \max_t \frac{\|\ddot{u}_m(t)\|}{\|\ddot{u}_m^{max}\|} \tag{35}$$

Downloaded From: https://www.spiedigitallibrary.org/conference-proceedings-of-spie on 15 Mar 2019
Terms of Use: https://www.spiedigitallibrary.org/terms-of-use

J_{14} defines the RMS of the maximum column curvature of the controlled structure, $\phi(t)$ divided by the RMS of the maximum uncontrolled column curvature:

$$J_{14} = \max_{t} \frac{\|\phi(t)\|}{\|\phi\|^{max}} \tag{36}$$

The following criteria evaluates the control system performance: J_{15} is the maximum control force of the controlled structure divided by the weight of the bridge structure, W.

$$J_{15} = \max_{t,i} \frac{|z_i(t)|}{W} \tag{37}$$

J_{16} is the maximum control device stroke, $u_z(t)$ divided by maximum bearing deformation $y_b^{max} = \sqrt{u_b^{max}}$.

$$J_{16} = \max_{t} \frac{|u_z(t)|}{y_b^{max}} \tag{38}$$

Performance criteria J_{17} maximum instantaneous power and J_{18} for maximum control power do not apply for this chapter since only semi-active control devices are implemented. Performance criteria J_{19} and J_{20} are the number of control and sensor devices, respectively.

6. RESULTS

The following section shows the results of the highway benchmark structure subjected to historical earthquakes. Initially, a parametric study was perform to obtain one design variable, β that would reduce base shear, overturning moment, mid-span displacement and mid-span acceleration. Figure 7 shows parametric study results performance criteria for maximum base shear (J1), overturning moment (J2), midspan displacement (J3), and acceleration (J4) with respect to the replicator dynamics parameters variations (Total available resources, P, ranging from 100 to 200 volts and growth rate value ranging from 0.001 to 20). This parametric study is a process require significant computational time and resources. Therefore, in this research the idea of using an optimization algorithm is advanced and NDAP is used to obtain the controller's replicator parameters.

NDAP model is investigated to simultaneously obtain 20 design variables for each control device (10 devices along the x-direction and 10 devices along the y-direction). The 20 sensor measurements are structural acceleration at those locations. NDAP is initialized with the following parameters:, $\theta_0 = [\beta_{ix}\beta_{iy}, \beta_{n+1}, P, f_{n+1}] = [18, ..., 18, 150, 0.001]$. The numerical integration for the Runge-Kutta solution is performed using the following parameters: $\alpha_0 = 0.01, \epsilon = 20$ and $n = 2$ and step size is $h = 0.01$. Each MR damper has a limiting maximum voltage of 10 Volts.

Figure 8 shows the variations of the 20 optimization variables (optimal replicator dynamics growth rate and total sum of the forces) for minimizing the acceleration objective function in x and y directions as a function of number of iterations for the structure subjected to El Centro earthquake obtained from NDAP. The optimal replicator parameter values for minimizing the acceleration objective function resulted in $\theta^* = [\beta_{ix}^*\beta_{iy}^*, \beta_{n+1}^*, P^*, f_{n+1}^*] = [17.24 to 19.5, 157, 0.0097]$. It is observed that the control devices along the x-axis require a higher value for growth rates, β_{ix}^*, compared with the control devices located along the y-axis, β_{iy}^*.

Figure 9 shows optimization iteration histories of the objective functions $F(\theta) = [F_1^x(\theta)F_1^y(\theta)F_2^x(\theta)F_2^y(\theta)]$ for the structure subjected to El Centro historical earthquake record when the accelerations objective functions are minimized using NDAP.

The proposed methodology effectively reduced the vibrations according to the performance criteria, but the competing objectives requires additional adjustments to obtain global minimum. Additional investigations with different objective functions is recommended, especially for multi-objective optimization problem to obtain Pareto-optimal design variables. Future work include the robustness evaluation and stability study using passitivity theorem of the control algorithm of the structure subjected to a wider range of historical earthquake accelerograms.

Downloaded From: https://www.spiedigitallibrary.org/conference-proceedings-of-spie on 15 Mar 2019
Terms of Use: https://www.spiedigitallibrary.org/terms-of-use

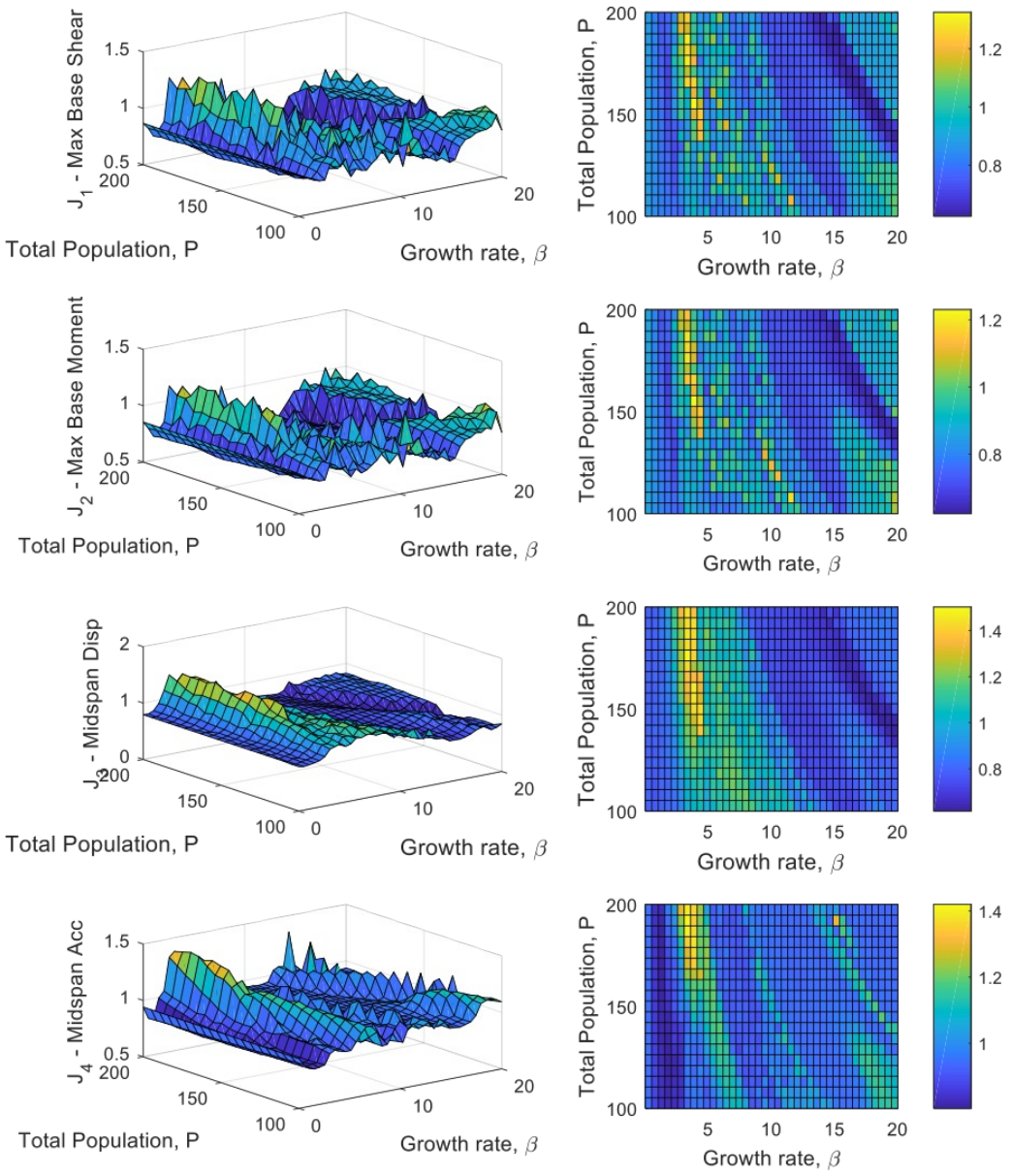

Figure 7. Performance criteria results for maximum base shear (J1), overturning moment (J2), midspan displacement (J3), and acceleration (J4)

7. CONCLUSION

This paper provided a new method for hybrid vibration control of base-isolated highway bridge structures using a bio-inspired control algorithm form evolutionary dynamics concept named replicator dynamics to determine control decisions in real-time. Additionally, a patented optimization model based on neural dynamics is investigated to obtain the control design variables for the replicator controller to reduce the vibrations of the bridge structure subjected to nonlinear constraints. An actual over-crossing 91/5 highway bridge in California is investigated. This benchmark problem is subjected to near-fault historical earthquakes to evaluate the performance of the controller using the 20 optimal control parameters obtained by NDAP.

Downloaded From: https://www.spiedigitallibrary.org/conference-proceedings-of-spie on 15 Mar 2019
Terms of Use: https://www.spiedigitallibrary.org/terms-of-use

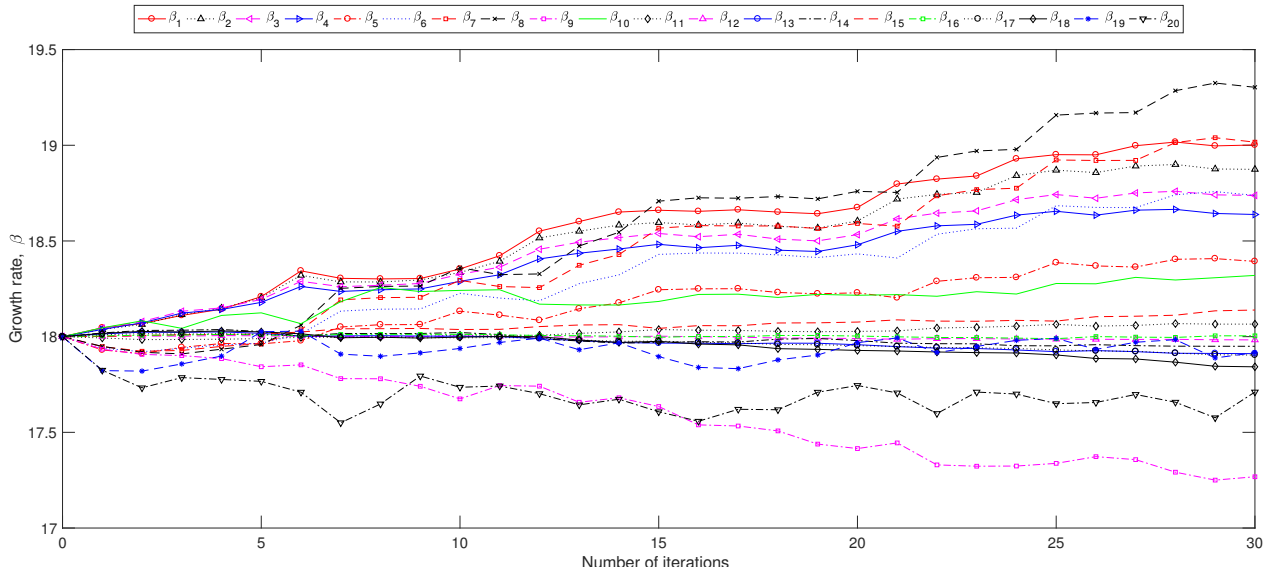

Figure 8. Variations of the optimization variables (optimal replicator dynamics growth rate and total sum of the forces) for minimizing the accelerations objective functions as a function of number of iterations for the structure subjected to El Centro earthquake record obtained from NDAP

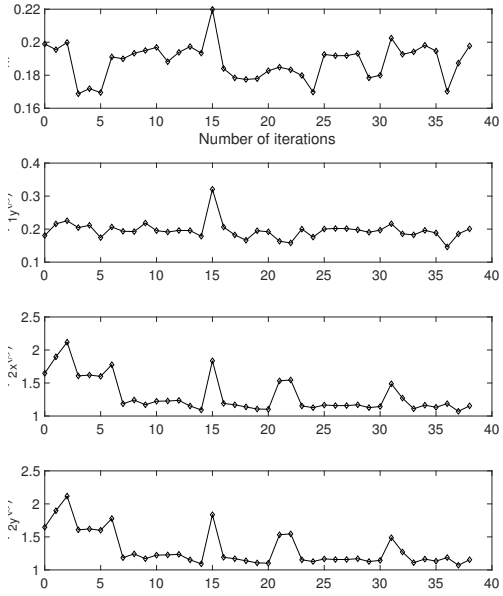

Figure 9. Optimization iteration histories of the objective functions of midspan displacement and mid-span accelerations $F(\theta) = [F_1^x(\theta)F_1^y(\theta)F_2^x(\theta)F_2^y(\theta)]$ of the structure subjected to El Centro historical earthquake record when accelerations along x and y are minimized using NDAP

REFERENCES

[1] G. Obando, A. P. and Quijano, N., "Building temperature control based on population dynamics," *IEEE Transactions on Control Systems Technology* **22**(1), 404 – 412 (2014).

[2] Gutierrez Soto, M. and Adeli, H., "Multi-agent replicator controller for sustainable vibration control of structures," *Journal of Vibroengineering* **19**(6), 4300–4322 (2017).

Downloaded From: https://www.spiedigitallibrary.org/conference-proceedings-of-spie on 15 Mar 2019
Terms of Use: https://www.spiedigitallibrary.org/terms-of-use

[3] Nowak, M. A., [*Evolutionary Dynamics: Exploring the Equations of Life*], Belknap Press of Harvard University Press, Cambridge, Massachusetts and London, England (2006).

[4] Adeli, H. and Park, H. S., "A neural dynamics model for structural optimization - theory," *Computers and Structures* **57**(3), 383 – 390 (1995).

[5] Park, H. S. and Adeli, H., "Distributed neural dynamics algorithms for optimization of large steel structures," *Journal of Structural Engineering* **123**(7), 880–888 (1997).

[6] Gutierrez Soto, M. and Adeli, H., "Many-objective control optimization of highrise building structures using replicator dynamics and neural dynamics model," *Structural and Multidisciplinary Optimization* **56**(6), 1521–1537 (2017).

[7] Gutierrez Soto, M. and Adeli, H., "Vibration control of smart base-isolated irregular buildings using neural dynamic optimization model and replicator dynamics," *Engineering Structures* **156**, 322–336 (2018).

[8] Makris, N. and Zhang, J.

[9] Agrawal, A., Tan, P., Nagarajaiah, S., and Zhang, J., "Benchmark structural control problem for a seismically excited highway bridgepart i: Phase i problem definition," *Structural Control and Health Monitoring* **16**(5), 509–529 (2009).

Downloaded From: https://www.spiedigitallibrary.org/conference-proceedings-of-spie on 15 Mar 2019
Terms of Use: https://www.spiedigitallibrary.org/terms-of-use